beta-Irradiation of pure 1-alkyl-3-methylimidazolium-based ionic liquids

Lehrhofer, Anna F.; Hosoya, Takashi; Hettegger, Hubert; Potthast, Antje; Rosenau, Thomas

Published in:
Cellulose

DOI:
10.1007/s10570-024-05932-7

Published: 01/06/2024

Document Version
Final published version

Document License
CC BY

Cellulose (2024) 31:5499–5511
https://doi.org/10.1007/s10570-024-05932-7

ORIGINAL RESEARCH

beta-Irradiation of pure 1-alkyl-3-methylimidazolium-based ionic liquids

Anna F. Lehrhofer · Takashi Hosoya · Hubert Hettegger · Antje Potthast · Thomas Rosenau

Received: 1 March 2024 / Accepted: 25 April 2024 / Published online: 7 May 2024

Abstract 1-Alkyl-3-methylimidazolium ionic liquids are common cellulose solvents and biomass pretreatment agents, while beta-irradiation ("e-beaming") is often used to decrease the recalcitrance of biomass towards hydrolysis or saccharification. Aiming at the general goal of elucidating the interaction between lignocellulosics, imidazolium-based ionic liquids, and beta-irradiation, we studied the effect of beta-irradiation on the pure ILs 1-ethyl-3-methylimidazolium and 1-butyl-3-methylimidazolium, both as chloride and acetate. Contrary to the expectation of inertness, irradiation caused degradation of the ILs, which was proportional to irradiation dosage, *i.e.*, to irradiation time and intensity. At a dosage of 2400 kGy, 0.2% (2000 ppm) of the IL were chemically altered. The main degradation pathway is the formation of imidazole and *N*-methylimidazole with concomitant dealkylation. The cleaved-off alkyl groups, apparently in cationic form, react with the anions present, accounting for the formation of alkyl chlorides and alkyl acetates from the chloride ILs and acetate ILs, respectively. A second, minor pathway comprises the degradation of the imidazole ring under conversion of the C_2-unit from the former C4-C5 moiety into ethylenediamine and reaction of the C_1-unit from the former C2 with the IL anions. Because of the non-neglible byproduct formation, the degradation of the ILs upon beta-irradiation and possible side reactions of the resulting byproducts need to be kept in mind for all setups that involve beta-irradiation and imidazolium ILs simultaneously.

A. F. Lehrhofer · H. Hettegger · A. Potthast · T. Rosenau (✉)
Department of Chemistry, Institute of Chemistry of Renewable Resources, University of Natural Resources and Life Sciences, Vienna (BOKU), Konrad-Lorenz-Strasse 24, A-3430 Tulln, Austria
e-mail: thomas.rosenau@boku.ac.at

T. Hosoya
Graduate School of Life and Environmental Sciences, Kyoto Prefectural University, Shimogamo-hangi-cho 11-5, Sakyo-ku, Kyoto-shi, Kyoto, Japan

H. Hettegger
Christian Doppler Laboratory for Cellulose High-Tech Materials, University of Natural Resources and Life Sciences, Vienna (BOKU), Konrad-Lorenz-Strasse 24, A-3430 Tulln, Austria

T. Rosenau
Faculty of Science and Engineering, Laboratory of Natural Materials Technology, Åbo Akademi University, Porthansgatan 3, FI-20500 Åbo/Turku, Finland

Graphical abstract

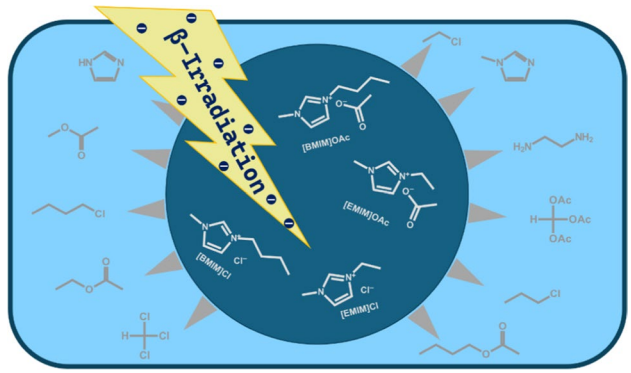

Keywords Beta-irradiation · Biomass pretreatment · Biorefinery · Cellulose · Imidazolium · Ionic liquids · Lignocellulose · Pulp

Introduction

In recent years, the convergence of biomass treatment strategies has become a focal point in the pursuit of efficient and sustainable biorefinery processes. Among the various methodologies, ionic liquids (ILs), mostly of the 1,3-dialkylimidazolium type, have emerged as agents in biomass pretreatment, demonstrating their remarkable ability to enhance accessibility, facilitate saccharification, and accelerate various downstream processes (Brandt et al. 2012; Zhang et al. 2021; Amini et al. 2021; Quesada-Salas et al. 2022; Meng et al. 2023; Roy et al. 2020; Roy and Chundawat 2023). However, the persisting challenges in IL purification and recycling have prompted researchers to explore innovative approaches that not only ensure effective biomass treatment but also address the recovery and reuse of ILs (Mora-Pale et al. 2011; Tu and Hallett 2019; Afonso et al. 2023).

Simultaneously, beta-irradiation, commonly referred to as "e-beaming", has gained prominence as a biomass pretreatment option, exhibiting favorable impacts on acidic and enzymatic hydrolysis for saccharification (Kumakura and Kaetsu 1983; Duarte et al. 2012; Shin and Sung 2008), on the accessibility of cellulosic pulps (Saeman et al. 1952; Ershov 1998; Dubey et al. 2004; Bouchard et al. 2006), on the reactivity in cellulose derivatization or generation of cellulose-bound metal nanoparticles (Iller et al. 2002; Ekman et al. 1984; Yokota et al. 2008) and on tuning the introduction of oxidized functionalities and the resulting depolymerization of polysaccharides (Henniges et al. 2012, 2013). Industrial electron accelerators operate in the low (80–300 keV), medium (300 keV-5 MeV), and high energy (above 5 MeV) ranges. Combined IL and beta-irradiation treatments have shown promising effects by enhancing hydrolysis rates, reducing tar content in biomass pyrolysis, and facilitating cellulose derivatization (Jusri et al. 2019; Zhang et al. 2021; Amini et al. 2021). These synergistic effects have been observed in diverse biomass treatment scenarios. If IL treatment is performed prior to beta-irradiation, it is difficult to ensure that the biomass is free of IL once it enters the irradiation phase, as the washing steps performed are rarely efficient enough to completely remove all IL residues. The presence of ILs during beta-irradiation, however, causes not only cellulose degradation (Hao et al. 2012) or crosslinking (Kimura et al. 2016) but also chemical derivatization of the lignocellulosic biomass under covalent incorporation of nitrogen (Jusner et al. 2023), alongside a macroscopic hydrophobization effect of wooden surfaces (Croitoru et al. 2014; Croitoru and Patachia 2016). The mechanisms and underlying chemistry of these processes are not yet understood and are the subject of current research. Thus, although the intersection of these two common "physical" biomass pretreatment methodologies has the potential for innovative applications, there is definitely an important "chemical" side that must not be neglected and needs to be understood in the first place.

This study addresses the question of whether chemical transformations take place during beta-irradiation of ILs and what the chemical structures of the possible degradation products are. We studied possible chemical effects of beta-irradiation in the idealized system of pure ionic liquids, as a first step towards more complex systems that contain also cellulose or other biomass. By bridging the knowledge gaps in the chemistry of the beta-irradiation/IL combination, this study hopes to contribute to purer and safer biomass treatment strategies and thus to greener and better-understood biorefinery practices.

Materials and methods

General

Commercial chemicals from Sigma-Aldrich/Merck (Schnelldorf, Germany) were of the highest grade available and were used without further purification. Solvents were purchased in synthesis grade from Roth, Sigma-Aldrich and VWR and were used as received. Distilled water was used for all aqueous solutions.

GC–MS/FID and UPC^2-ESI-QTof-MS analyses were performed as previously described by Barbini et al. (2021a, b). UV/Vis spectra were recorded on a LAMBDA 45 UV/Vis spectrophotometer (Perkin Elmer, Waltham, MA, USA): range of 400 to 700 nm, scanning speed 480 nm min^{-1}, quartz glass cuvettes (l = 1.0 cm).

beta-Irradiation

beta-Irradiation (electron beam irradiation) was carried out at NHV Corporation (Kyoto, Japan) on a Curetron® EBC300-60 electron beam generator at 300 keV, and at Kremsmünster (Austria) on a Rhodotron IBA TT-100 accelerator at 10 MeV. The samples were irradiated in quartz cuvettes (100 cm^2, thickness 2 mm) equipped with a gas-tight septum. The samples were irradiated at dosages between 60 and 2400 kGy (30.7 mA). For detailed procedures see Ehrhardt et al. (2005) and Henniges et al. (2012, 2013). Cellulose sources were available from previous work: bacterial cellulose (Sulaeva et al. 2020), cellulose II gels from Lyocell processing (Beaumont et al. 2017).

Gas chromatographic analysis (GC–MS/FID)

For the procedure see Becker et al. (2013). An Agilent 5975C instrument with an inert XL TAD MS detector and FID was used, with a synchronized recording of FID and MS (splitter: one third of the flow to MS, two thirds to FID). The MS trace was used for identification, while the FID trace was used for additional identification in spiking runs (to avoid overloading the MS detector). MS detector: EI mode, 70 eV, source pressure: $1.13 \cdot 10^{-7}$ Pa, source temperature: 230 °C. The mass scanning range was set at 29–1050 amu, without solvent cutting time to be able to detect the very volatile methyl and ethyl derivatives. FID: 280 °C, with a H_2 flow of 30 mL min^{-1}, air flow of 400 mL min^{-1}, and makeup flow (combined) of 25 mL min^{-1}. Separation: DB-5ht capillary column (30 m × 250 µm × 0.1 µm, J&W Scientific, Folsom, CA, USA); carrier gas: helium; column flow: 0.9 mL min^{-1}; purge flow: 32.4 mL min^{-1}; oven program: 50 °C (2 min), 5 °C min^{-1}, 280 °C (20 min). Injection: 1.0 µL; autosampler with a multimode inlet (MMI) kept at 280 °C. The split ratio was set to 15:1 at a split flow of 37.5 mL min^{-1}. The total analysis time was 45 min. MS data collection and processing: Enhanced ChemStation (MSD Chemstation F.01.01.2317) and MassHunter Workstation software. The compounds were identified by comparison with the Wiley10 and NIST11 mass spectral libraries.

Pertrimethylsilylation

In parallel, GC analysis after trimethylsilylation was carried out. A 10 µL amount of the solvent-free extract was dissolved in anhydrous pyridine (200 µL) containing 300 µg mL^{-1} of DMAP as a silylation catalyst. BSTFA (120 µL) was added, the mixture was heated to 70 °C for 2 h, cooled to RT, and immediately analyzed. The sample was kept in the dark in a tightly closed vial at -80 °C.

Headspace GC–MS

GC/MS analysis was carried out on an Agilent 6890N gas chromatograph equipped with a 5975 B mass spectrometer, a split/splitless inlet, and an Agilent 7697A closed-loop headspace sampler. Separation: column: GS-GasPro (30 m × 0.25 mm i.d. × 0.25 µm film thickness; J&W Scientific,

Folsom, CA, USA); split/splitless inlet parameters: constant flow at 11.2 mL min^{-1}; carrier gas: He; split: 10:1; injector: 250 °C; temperature profile: 5 °C (4 min), 10 °C min^{-1} to 200 °C (5 min) and back to initial values; MSD transfer line temperature: 250 °C; MS source and MS quadrupole temperature: 230 °C and 150 °C, respectively. Headspace injection: vial temperature: 50 °C; loop temperature: 95 °C; transfer line temperature: 110 °C; vial equilibration time: 10 min; vial pressurization time: 0.2 min; loop fill time: 0.5 min; loop equilibration time: 0.2 min; loop size: 1 mL; and injection time: 1 min. Data acquisition was done in scan mode, scan parameters: low mass: 32 m/z; high mass: 550 m/z. A liquid nitrogen cooling system for the gas chromatograph was used; such a low starting temperature was necessary to ensure reliable separation of methyl chloride, ethyl chloride and methyl acetate. The system was operated with MassHunter GC/MS software (Agilent Technologies Inc.). MSD ChemStation software (Agilent Technologies Inc.) was used for data processing.

Extraction of IL-degradation products by supercritical CO_2

Supercritical extraction of the irradiated ILs was carried out with carbon dioxide (> 99.5% food grade, Biogon C, Linde AG, Austria) on a high-pressure SF-1 supercritical fluid system (Separex, Champigneulles, France) equipped with preheater, autoclave, and separator. The irradiated IL (200 mL) was extracted stationary without flow for 10 min and for another 10 min at a flow rate of 30 g min^{-1}. Extraction proceeded at 30 MPa (300 bar) and 40 °C (ρ CO_2: 910 kg m^{-3}) in a cylindrical extraction vessel (Ø: 35 mm, height: 50 mm). *n*-Heptane (3 wt%) ($\rho_{22\ °C}$: 684 kg m^{-3}, Merck) was added as a co-solvent by an HPLC pump (Lab Alliance) to avoid volatilization of the compounds which are gases under standard conditions upon depressurization. The extracts were stored under argon gas at -80 °C in brown-glass vials.

NMR analysis

Solution-state NMR spectra were recorded using a Bruker Avance II 400 spectrometer equipped with a cryogenically-cooled broadband observing (BBO) 5 mm probe-head (CryoProbe™ Prodigy, N_2-cooled). The NMR experiments were performed with z-gradients at RT at resonance frequencies of 400.13 MHz for ^{1}H, 100.61 MHz for ^{13}C, and 40.54 MHz for ^{15}N using standard Bruker pulse programs. Chemical shifts are given in parts per million (ppm) and were referenced to the respective residual solvent signal (DMSO-d_6; 2.50 ppm for ^{1}H, 39.52 ppm for ^{13}C). ^{1}H NMR spectra were recorded with 32 k complex data points and apodized using a Gaussian window function (lb = -0.30 Hz and gb = 0.30 Hz) prior to *Fourier* transformation. ^{13}C NMR *J-modulated* spectra using WALTZ16 ^{1}H decoupling (Bruker pulse program "*jmod*") were recorded with 65 k complex data points. S/N was enhanced utilizing an exponential window function (lb = 1.0 Hz) before *Fourier* transformation. ^{1}H-^{1}H COSY using gradient pulse for selection (Bruker pulse program "*cosygpqf*") was used to determine homonuclear shift correlation and acquired with 2048 × 256 data points. The multiplicity-edited HSQC experiment (Bruker pulse program "*hsqcedetgpsp.3*") was performed using adiabatic pulses for inversion of ^{13}C and GARP-sequence for broadband ^{13}C-decoupling, optimized for $^{1}J(CH) = 145$ Hz and acquired with 1024 × 256 data points. For determination of long-range ^{1}H-^{13}C couplings, the HMBC experiment using gradient pulses and a low-pass filter without decoupling (Bruker pulse program "*hmbcgplpndqf*") was performed and acquired with 1024 × 256 data points. To determine ^{1}H-^{15}N couplings, a ^{1}H-^{15}N HMBC experiment (Bruker pulse program "*hmbcgplpndqf*") was performed acquiring 1048 × 128 data points; ^{15}N shifts were extracted from the obtained 2D spectra. All NMR data was acquired and processed using Bruker TopSpin 4.3.0 and/or 3.2.7 software.

For NMR data of the identified compounds (**5**–**15**) see Table 2.

Computations

The GAUSSIAN09 software (Frisch et al. 2016) was employed in all calculations. The DFT(M06-2X) level of theory was applied for geometry optimization, frequency calculation, and energy evaluation throughout this study, with the 6-311G(d,p)

basis sets for C, O, H, Cl, and N, with diffuse functions being added to C, O, Cl, and N. It was ascertained that each equilibrium geometry exhibited no imaginary frequency. Changes in enthalpy, entropy, and Gibbs energy were calculated for 298.15 K.

Results and discussion

Extraction of degradation products

To keep the system under study as simple as possible in the beginning, this study focuses on pure ionic liquids – without any solute or biomass components being present. We used the common ILs 1-ethyl-3-methylimidazolium and 1-butyl-3-methylimidazolium, both as chloride and acetate, see Scheme 1. To confirm whether or not beta-irradiation of such pure ILs triggers any chemical processes, a method is required to separate these putative products, which are likely to be present in trace amounts only, from the large excess of the bulk IL. Conventional extraction with IL-immiscible organic solvents was unsuccessful since the extractants always contained traces of IL, which – upon gas chromatographic (GC) analysis – were deposited in the GC liner and capillary and permanently compromised the capillary´s and the whole system´s performance. Similarly, the electrochemical detector in ion chromatography also seemed to be affected by the trace quantities of ILs present, because a loss in response was observed over time. Even the otherwise quite robust HPTLC technique (*cf.* Böhmdorfer et al. 2018) is affected by traces of ILs in the sample, which decrease the UV response of monosaccharides in hydrolysates of carbohydrates. The issue of trace ILs causing analytical problems in GC and IC practice will be addressed in more detail in an upcoming account. For these reasons, approaches using organic solvents for IL extraction were not further pursued: the possible interference of IL traces with analytical techniques seemed rather unpredictable and – at least in the case of permanently damaged GC capillaries – too severe.

Taking advantage of the often-described negligibly small vapor pressure of the ILs, which prevents the IL from entering the gas phase, we used headspace GC analysis of the gas phase for the detection of possible volatiles, in combination with evaporation of dissolved byproducts under reduced pressure (0.15 bar) and recovery in a cryotrap (-48 °C, acetone/dry ice) filled with diethyl ether. Through simultaneous purging of the IL with a minute stream of inert gas (Ar) during the evaporation, the setup was, in principle, similar to that of a vacuum distillation.

As a complementary separation method, extraction with supercritical carbon dioxide ($scCO_2$) was carried out after headspace sampling of the gas phase, using a previously established setup (Barbini et al. 2021a, b). Some ILs, although generally ionic and very polar, are able to dissolve the highly apolar $scCO_2$ (Jutz et al. 2011; Keskin et al. 2007; Blanchard et al. 2001). Lipophilic moieties, *e.g.*, long alkyl chains in anions and/or cations, thereby promote the $scCO_2$ uptake. By contrast, the $scCO_2$ phase remains immiscible with ILs that lack such apolar substituents, with the four ILs applied in this study, 1-ethyl-3-methylimidazolium and 1-butyl-3-methylimidazolium, both

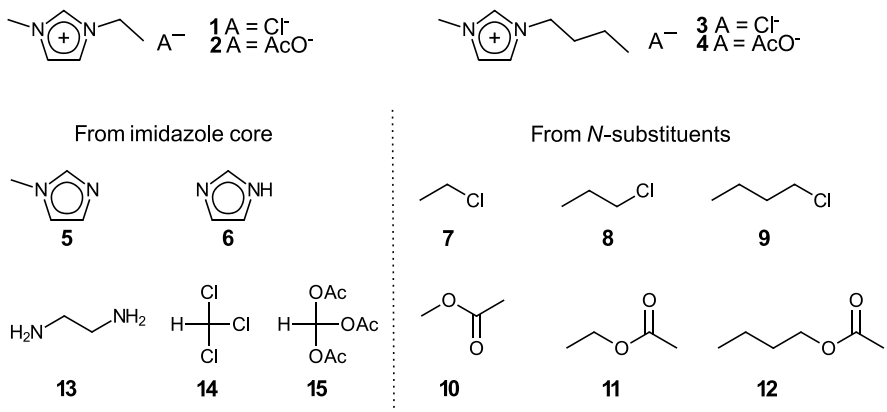

Scheme 1 Chemical structures of the 1-alkyl-3-methylimidazolium-based ionic liquids used (**1**–**4**) and their detected degradation products (**5**–**15**) formed upon extensive beta-irradiation

as chloride and acetate, respectively, being completely $scCO_2$-insoluble (Aki et al. 2004; Kazarian et al. 2000; for a comprehensive overview on the interplay between ILs and $scCO_2$ see the recent summary by Martinez 2023). This phase behavior eliminated the danger of IL traces in the extracts interfering with instrumental analysis and rendered $scCO_2$ extraction a viable alternative to the distillative removal of the degradation products. Both separation methods, vacuum distillation and $scCO_2$ extraction, provided the same results, with the exception that some of the rather volatile compounds that are gaseous under standard conditions were detected in smaller amounts with the $scCO_2$ approach (sweeping out by CO_2) compared to distillation/cryotrapping.

N-Methylimidazole (MIm), imidazole (Im), and – in many instances – water, are nearly ubiquitously occurring trace impurities in 1-alkyl-3-methylimidazolium liquids, stemming either from the IL synthesis itself or degradation and aging processes (Liebner et al. 2010). We recently showed the occurrence and involvement of Im and MIm in the case of cellulose or lignocellulose being beta-irradiated in the presence of EMIM or BMIM ILs (Jusner et al. 2023). For the study of the irradiation effect on the IL, it was necessary to exclude the presence of Im and MIm traces to rule out any side reactions and catalytic effects of these byproducts. We used the sequence of drying over neutral alumina (Brockmann grade 1) to remove water, followed by $scCO_2$ extraction to remove MIm/Im traces, and a final vacuum treatment (5 min, 0.15 bar) at RT. In addition to removing water, Im and MIm, this procedure also guaranteed that the IL was free from dissolved oxygen so that autoxidation processes and any formation of reactive oxygen species was minimized or even fully prevented. Thus, both the purification of the starting IL and the collection of possible degradation products used in principle the same extraction method with $scCO_2$.

After irradiation, IL degradation ranged between approx. 400 ppm at 400 kGy to about 2000 ppm at 2400 kGy, quantified as the mass sum of the extracted degradation products, *i.e.*, as the mass difference of the IL before and after irradiation / extraction (Fig. 1). As blank runs, extraction of the purified ILs without irradiation was performed. In these cases, no compounds were extracted and the extracted mass was zero. The results for the irradiated ILs were astonishingly consistent, with minimal differences between the four ILs, although it should be noted that the measurements of the sum of the extracted compounds only provided approximative values as the primary extracts contain very volatile compounds. The mass was therefore determined after equilibration at RT and ambient pressure (1 h) and does not comprise the very volatile constituents, which had been determined by headspace-GC beforehand. Apart from this limitation, the overall masses of formed degradation products showed a clear correlation with irradiation dosage time at constant intensity and irradiation intensity at constant time, the formation of byproducts thus being a function of the irradiation

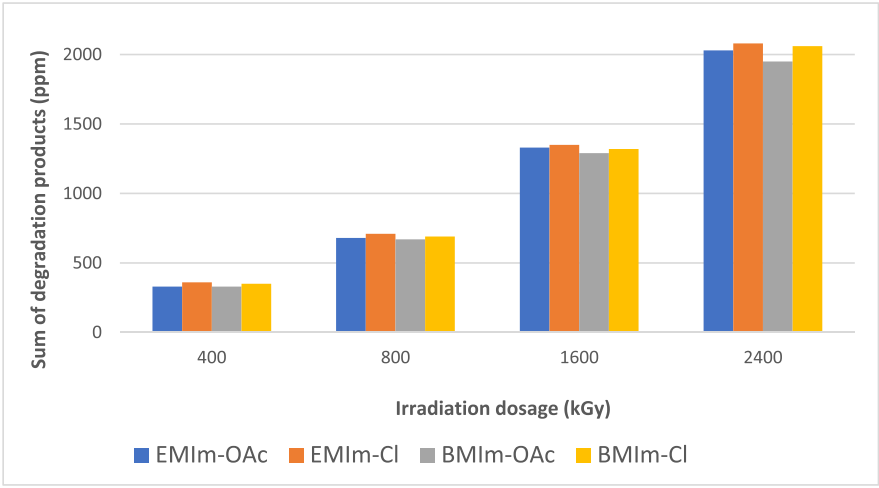

Fig. 1 Degradation of pure ILs by beta-irradiation depending on the irradiation dosage, measured as the sum of degradation products (mass loss of IL after irradiation and extraction)

Table 1 Degradation products formed upon beta-irradiation of 1-alkyl-3-methylimidazolium ILs, identified by NMR and GC–MS. XXX = major product, XX = product, X = trace product

Degradation product	From EMIM-Cl	From EMIM-OAc	From BMIM-Cl	From BMIM-OAc
N-Methylimidazole (**5**)	XXX	XXX	XXX	XXX
Imidazole (**6**)	XXX	XXX	XXX	XXX
Chloromethane (**7**)	XX		XX	
Chloroethane (**8**)	XX			
1-Chlorobutane (**9**)			XX	
Methyl acetate (**10**)		XX		XX
Ethyl acetate (**11**)		XX		
Butyl acetate (**12**)				XX
Ethylenediamine (**13**)	X	X	X	X
Chloroform (**14**)	X		X	
Triacetoxymethane (**15**)		X		X

dosage (see Fig. 1). Dosage D[1] is expressed in Gy or kGy, which is defined as the absorbed energy (J) per mass of irradiated matter (kg), its unit thus being J/kg = Nm/kg = (kg·m/s^2)/kg = m^2/s^2.

Identification of degradation products

The identified degradation products formed in the four ILs (**1**–**4**) upon beta-irradiation (1020 kGy) are shown in Scheme 1, while Table 1 categorizes the degradation products (**5**–**15**) according to the IL compounds from which they originate. Table 2 lists relevant analytical and spectroscopic compound data of the degradation products, along with the NMR data with full resonance assignment in the ^{1}H and ^{13}C domains and the mass spectra (70 eV, electron impact) as obtained upon GC–MS separation.

Evidently, the formed alkyl chlorides can only originate from imidazolium chloride ILs (**1**, **3**), and the alkyl acetates (acetic acid esters) from the imidazolium acetate ILs (**2**, **4**). MIm (**5**), Im (**6**), and small amounts of ethylenediamine (**13**) were found in all four ILs. While the latter three compounds originate from the degradation of only the imidazolium cation structure, alkyl chlorides and alkyl acetates involve both cation fragments (alkyl chains) and anions (chloride, acetate). In general, the molar sum amount of alkyl derivatives (methyl and ethyl/butyl) corresponded roughly to the sum of MIm and Im formed, as they originate from the 1,3-dialkylimidazolium moiety as mutual precursor. The concentration of **13** + **14** in the chloride case (or **13** + **15** in the acetate case) was about significantly smaller (roughly 10% w/w) than that of the other products, indicating a different, minor degradation pathway.

Mechanistic considerations

Regarding the degradation mechanism, two principal classes of pathways can be distinguished according to the type of products formed. The first, major group of reactions was obviously an *N*-dealkylation, involving both the *N*-methyl and the *N*-alkyl groups. Formally, the *N*-substituents must be cleaved off as cations in order to recombine with the IL anions to form alkyl chlorides with Cl^- and alkyl acetates (acetic acid alkyl esters) with AcO^-. Apparently, these processes are rather fast since in the case of the *n*-butyl derivatives no rearrangement products (*iso*-, *sec*- or *tert*-butyl derivatives) were found.

The second, minor group of reactions causes far-reaching fragmentation of the IL cations: the C4-C5 unit stays intact and remains bound to the two nitrogen atoms, and C-2 is cleaved off and reacts with the nucleophilic anions present. The C_2-unit (C4-C5) is reduced in this process, its former double-bonded C–C structure now being present as ethylenediamine (1,2-diaminoethane, **13**). This cation fragmentation

[1] With the irradiance intensity I (units: [W/m^2] = [kg*m/s^3)/m^2]) we obtain: dosage D = I*t*V/m (units: [kg*m/s^3)/m^2*s*m^3/kg] = [m^2/s^2]).

Table 2 Analytical and spectroscopic data of the products formed upon beta-irradiation of 1-alkyl-3-methylimidazolium ILs. MS: EI(+), 70 eV, *m/z*. NMR: DMSO-d_6, ^{1}H: 400.13 MHz, ^{13}C: 100.61 MHz, δ in ppm, *J* in Hz

Degradation product	Compound data	Analytical data (NMR, MS)[a]
N-Methyl-imidazole (**5**)	$C_4H_6N_2$, 82.104 g mol^{-1}, b.p. = 198 °C CAS: 616–47-7	NMR: ^{1}H: δ 7.56 (bs, 1H, 2-CH), 7.09 (t, 1H, *J* = 1.23, 4-CH), 6.89 (t, 1H, *J* = 1.23, 5-CH), 3.63 (s, 3H, N-CH_3); ^{13}C: δ 137.9 (2-CH), 128.4 (4-CH), 120.4 (5-CH), 32.69 (N-CH_3); MS: 82 (100), 81 (15), 55 (10), 54 (20), 42 (25), 41 (15), 40 (15), 28 (15), 15 (10)
Imidazole (**6**)	$C_3H_4N_2$, 68.077 g mol^{-1}, b.p. = 256 °C CAS: 288–32-4	NMR: ^{1}H: δ 12.07 (bs, 1H, NH), 7.64 (s, 1H, 2-CH), 7.02 (bs, 2H, 4-CH, 5-CH); ^{13}C: δ 135.2 (2-CH), 127.6 (4-CH), 115.8 (5-CH); MS: 68 (100), 67 (10), 41 (55), 40 (35), 39 (10), 28 (25)
Chloromethane (**7**)	CH_3Cl, 50.488 g mol^{-1}, b.p. = -24.2 °C CAS: 74–87-3	NMR:[b] ^{1}H: δ 3.05 (s, 3H, CH_3), 1.47 (t, 3H, *J* = 7.22, CH_3); ^{13}C: δ 25.8 (CH_3); MS: 52 (30), 50 (100), 35 (10), 15 (75)
Chloroethane (**8**)	C_2H_5Cl, 64.514 g mol^{-1}, b.p. = 12.3 °C CAS: 75–00-3	NMR:[b] ^{1}H: 3.54 (q, 2H, *J* = 7.22, CH_2), 1.47 (t, 3H, *J* = 7.22, CH_3); ^{13}C: δ 40.0 (CH_2), 18.8 (CH_3); MS: 66 (35), 64 (100, M^+), 49 (20), 29 (70), 28 (85), 27 (60)
1-Chlorobutane (**9**)	C_4H_9Cl, 92.567 g mol^{-1}, b.p. = 78 °C CAS: 109–69-3	NMR: ^{1}H: δ 3.62 (t, 2H, *J* = 6.62, 1 CH_2), 1.69 (m, 2H, *J* = 6.73, 2-CH_2), 1.31 (m, 2H, *J* = 6.73, 3-CH_2), 0.89 (t, 3H, *J* = 7.40, CH_3); ^{13}C: δ 45.10 (CH_2Cl), 34.08 (2-CH_2), 19.52 (3-CH_2), 13.17 (CH_3); MS: 92 (2, M^+), 56 (100), 43 (25), 41 (55)
Methyl acetate (**10**)	$C_3H_6O_2$, 74.078 g mol^{-1}, b.p. = 57.1 °C CAS: 79–20-9	NMR: ^{1}H: δ 3.57 (s, 3H, OCH_3), 2.00 (s, 3H, CH_3 in Ac); ^{13}C: δ 170.8 (CO), 51.19 (OCH_3), 20.40 (CH_3 in Ac); MS: 74 (30), 59 (15), 43 (100), 42 (15), 29 (10), 15 (10)
Ethyl acetate (**11**)	$C_4H_8O_2$, 88.105 g mol^{-1}, b.p. = 77.1 °C CAS: 141–78-6	NMR: ^{1}H: δ 4.03 (q, 2H, OCH_2), 1.98 (s, 3H, CH_3 in Ac), 1.18 (t, 3H, CH_3 in Et); ^{13}C: δ 170.2 (C = O), 59.70 (OCH_2), 20.69 (CH_3 in Ac), 14.04 (CH_3 in Et); MS: 88 (10), 70 (10), 61 (15), 45 (15), 43 (100), 29 (15), 15 (10)
Butyl acetate (**12**)	$C_6H_{12}O_2$, 116.16 g mol^{-1}, b.p. = 126 °C CAS: 123–86-4	NMR: ^{1}H: δ 3.99 (t, 2H, *J* = 6.64, 1-CH_2), 1.99 (s, 3H, CH_3 in Ac), 1.54 (m, 2H, *J* = 7.73, 2-CH_2), 1.31 (m, 2H, *J* = 7.73, 3-CH_2), 0.88 (t, 3H, *J* = 7.38, 4-CH_3); ^{13}C: δ 170.4 (CO), 63.47 (1-CH_2), 30.21 (2-CH_2), 20.70 (CH_3 in Ac), 18.64 (3-CH_2), 13.50 (4-CH_3); MS: 115 (2), 87 (5), 73 (20), 61 (15), 56 (35), 43 (100), 41 (20), 29 (15), 27 (15), 15 (10)
Ethylenediamine (**13**)	$C_2H_8N_2$, 60.098 g mol^{-1}, b.p. = 116 °C CAS: 107–15-3	NMR: ^{1}H: δ 2.47 (s, 4H, 2xCH_2), 1.30 (bs, 4H, 2xNH_2); ^{13}C): δ 45.18 (CH_2); MS: 60 (10), 59 (10), 43 (15), 42 (15), 30 (100), 28 (20)
Chloroform (**14**)	$CHCl_3$, 119.38 g mol^{-1}, b.p. = 61.2 °C CAS: 67–66-3	NMR: ^{1}H: δ 7.29 (s, 1H, CH); ^{13}C: δ 79.14 (CH); MS: 87 (15), 85 (75), 83 (100), 49 (10), 48 (15), 47 (30), 35 (10)
Triacetoxymethane (**15**)	$C_7H_{10}O_6$, 190.05 g mol^{-1}, b.p.: 28 °C CAS: 174–11-4	NMR:[b] ^{1}H: δ 5.28 (s, 1H, CH), 1.98 (s, 9H 3 × CH_3 in Ac); ^{13}C: δ 171.4 (CO), 114.4 (CH), 20.6 (CH_3 in Ac); MS: 190 (10), 147 (15), 104 (15), 88 (35), 43 (100), 29 (20), 15 (10)

[a]MS comparison: NIST database 2023

[b]measured in $CDCl_3$

seems to occur during or after double *N*-dealkylation – otherwise, *N*-substituted derivatives of ethylenediamine should have been found as well. If double *N*-dealkylation (*i.e.*, formation of imidazole **6**) precedes the fragmentation, as hypothesized, an IL spiked with imidazole should exhibit increased contents of ethylenediamine (**13**) and products of C-2 (**14**, **15**) upon irradiation treatment. However, when irradiating EMIM-Cl (**1**) containing 3% Im (**6**), no larger amounts of ethylenediamine (**13**) and chloroform (**14**) were detected than in the case of the pure starting IL. This supports a fragmentation

mechanism in which double *N*-dealkylation and ring fragmentation of the 1-alkyl-3-methyl-imidazolium cations occur simultaneously, quasi concertedly, rather than in a fragmentation process starting from Im (i.e., doubly *N*-dealkylated IL). It should be noted that the reduction of the C–C double bond in imidazolium is formally a hydrogenation that requires hydrogen (protons plus electrons), of which the source remains unclear.

Regarding the chemical degradation processes as a consequence of beta-irradiation, relatively few mechanistic details are known apart from the fact that beta-irradiation is classified as ionizing irradiation and causes chemical bond cleavage in organic materials. This is used in various applications, such as sterilization of medical equipment, crosslinking of polymers, and human cancer therapy (Märk and Dunn 2013). beta-Irradiation can have a wide energy spectrum from a few eV in cathode rays – an energy of 70 eV is the standard for electron impact ionization in mass spectrometry – up to several MeV in the beta-decay of radioactive nuclei. Generally, the electrons, when entering matter and interacting with it, cause electron cascades. In this process, the electron knocks out one or more further electrons from the electron shells of the atoms. The secondary electrons are lower in energy, but still energetic enough to knock out further electrons. Consequently, a cascade occurs until the energy of the incident electrons is too low for further ionization. When the electron collides with a molecule, the sample molecule is ionized or fragmented. These processes are, in principle, known from electron impact (EI) ionization in mass spectrometry (Mirsaleh-Kohan et al. 2008; Cappiello et al. 2001) which, however, uses the well-defined, quite low energy of 70 eV to obtain high ionization of molecules M, with only moderate fragmentation, and highly reproducible fragmentation patterns, the fundamental process being: $M + e^- \rightarrow M^+ + 2\ e^-$. By contrast, bond cleavages as a consequence of higher-energy beta-irradiation (with an energy around 1 MeV) are more likely to be random and hard to predict, because the energy of the primary and secondary electrons covers a very wide energy range.

After irradiation of the IL samples (**1**–**4**), spin-trapping of possible C-, N-, or O-centered radicals with the radical trapping agent EMPO (Stolze et al. 2003) revealed no trappable homolytic intermediates and no indication of the presence of any reasonably long-lived radical intermediates. Further, no *N*-chlorination or elemental chlorine – the product of the recombination of two chlorine radicals – was observed for the chloride-type ILs. This seemed to point toward the direction of a non-homolytic formation path for the observed degradation products. Assuming processes that are in principle similar to EI ionization, the 3-alkyl-1-methylimidazolium cation – with the alkyl residue R being ethyl or butyl in the present case – would undergo fragmentation in which one of the *N*-alkyl-substituents is lost as an alkyl cation (*i.e.*, a carbenium ion). The preferred follow-up process is evidently its recombination with the anions present in large access. This accounts for the observed predominance of alkyl chlorides (from **1** and **3**) and alkyl acetates (from **2** and **4**) in the degradation mixtures, apart from *N*-methylimidazole (**5**). The elimination of the second *N*-alkyl substituent would follow a similar mechanism, giving another alkyl chloride/alkyl acetate and imidazole (**6**).

The product distribution in the degradation mixtures (Table 1) allows two interesting conclusions. First, the first *N*-dealkylation step is always the loss of the larger *N*-substituent (ethyl or butyl), but not the loss of the *N*-methyl group, because exclusively *N*-methylimidazole (**5**) was detected as the primary *N*-dealkylation product, but no *N*-ethylimidazole (from EMIM) or *N*-butylimidazole (from BMIM), respectively. Second, the fact that *N*-methylimidazole and imidazole are formed in nearly equal amounts demands that the *N*-demethylation of *N*-methylimidazole (**5**) proceeds much faster than the first dealkylation of the 3-alkyl-1-methylimidazolium cations. If we assume comparable dealkylation rates for 3-alkyl-1-methylimidazolium and methylimidazole, almost no imidazole would be formed in the irradiation system because the concentration of *N*-methylimidazole as the starting material for further dealkylation and imidazole formation would be extremely low. At an average concentration of 1000 ppm of MIm over the irradiation time, the rate of *N*-dealkylation of MIm would have to be 1000 times higher than that of *N*-dealkylation of the 3-alkyl-1-methylimidazolium cations to account for the roughly equal amounts of MIm and Im actually produced.

To suggest a "chemical" mechanism for the formation of the other trace products found, *i.e.*, the ethylenediamine (**13**, C_2-unit, former C-4 and C-5) and the substituted C_1-unit (former C-2) from the imidazole

core, one cannot go much beyond conjecture, given the high-energy regime of beta-irradiation. As indicated above, double *N*-dealkylation must have preceded the ethylenediamine formation as both of its NH_2-groups were unsubstituted. The source of the reduction equivalent and the hydrogen (protons) required for reduction are unknown. The former C-2 reacted as formal trication equivalent or formal orthoformic acid ($HC(OH)_3$) synthon, binding three anion equivalents – either chloride to give $HCCl_3$ (**14**) or acetate to afford $HC(OAc)_3$ (**15**). As well-known as the former compound is, as rare is the latter: triacetoxymethane can be formally regarded as a triply mixed anhydride of orthoformic acid and acetic acid. Synthetically, it is available in moderate yields by *Willamson*-type synthesis from trihalomethanes and lithium acetate or almost quantitatively by ozonolysis of tri(isopropylenoxy)methane. The formation of the two compounds **14** and **15** is interesting insofar as they incorporate both a fragment of the former IL cation and more than one IL anion.

We currently conduct computations on the DFT (M06-2X) level to shed some more light on the reaction pathways leading to the observed degradation products. The starting points are the EMIM dication and the MIm cation, produced by electron impact on the EMIM cation and MIm, respectively. Computations of the heterolytic bond energies confirm that the N–C bonds between the ring nitrogen and the *exo*-alkyl group are by far the weakest link in the system and thus most prone to elimination (as alkyl cation). The heterolytic bond energy is made up of the homolytic binding energy, the ionization energy of one radical formed and the electron affinity of the other radical. Also the stability difference between the C-N bond in *N*-butyl (or *N*-ethyl) relative to *N*-methyl agreed with the observed easier dealkylation of the *N*-alkyl (butyl, ethyl) substituent relative to the *N*-methyl group. Details of the computed pathways and compound stabilities will be communicated in due course.

Conclusions

In conclusion, our study has demonstrated the unexpected degradation of 1-alkyl-3-methylimidazolium ionic liquids (ILs) upon beta-irradiation, contrary to initial assumptions of their inertness being more pronounced. The degradation process is dose-dependent, with the main pathway involving *N*-dealkylation and subsequent reactions of the cleaved alkyl groups with the anions present in the ILs. Alkyl chlorides and alkyl acetates are formed from chloride and acetate ILs, respectively. Additionally, a minor pathway results in the degradation of the imidazole ring, yielding ethylenediamine as a C_2-unit. The study also briefly addressed the challenges in analytical methods to detect trace analytes in the bulk ILs and the resulting choice of separation methodology: the degradation products were efficiently separated from the IL phase using either a combination of headspace gas analysis and evaporation under reduced pressure with recovery in a cryotrap and alternatively the extraction with supercritical carbon dioxide.

Our findings emphasize the importance of considering the degradation of ILs in biorefinery setups involving beta-irradiation and cellulose or other polysaccharides present. While the reaction of imidazolium ILs with cellulose or other polysaccharides is well studied, the effect of beta-irradiation on the ILs alone is quite surprising – apart from the fact that small amounts of the IL are consumed and degraded, there might be chemical effects of the cleavage products which need to be considered additionally. Imidazole and *N*-methylimidazole, for instance, generate basic conditions prone to triggering beta-alkoxy-elimination, which, in turn, results in chain degradation of oxidatively damaged celluloses (Hosoya et al. 2018) or in condensation reactions causing chromophore formation and yellowing (Korntner et al. 2015). The presence of the formed basic compounds (MIm, Im) and alkyl chlorides (**7**–**9**) as alkylating agents might cause low-degree alkylation of polysaccharides present. Similarly, triacetoxymethane (**15**) is a very potent acetylating agent that might cause low-degree acetylation of cellulose – a process that even occurs (without beta-irradiation) in cellulose solutions in EMIM-OAc or BMIM-OAc (Zweckmair et al. 2015), but would obviously be enhanced when exposed to beta-irradiation additionally. The combination of acetic acid and imidazole exerts a strongly acetylating action via intermediate *N*-acetylimidazole (Beaumont et al. 2020, 2021), even in aqueous media, which needs to be kept in mind when cellulose is present. Furthermore, ethylenediamine (**13**) is known to be integrated into the crystalline structure of cellulose I to form its own allomorph,

"ethylenediamine-cellulose I" (Nishiyama et al. 2010), which would account for the incorporation of nitrogen into cellulose. Fixated in this form, ethylenediamine would behave as if covalently bound and would not be removable by washing (Qin et al. 2015; Jusner et al. 2023).

Although the amount of the formed degradation products is rather small (0.2 wt% at 2400 kGy), it must be kept in mind that the formed alkyl chlorides (**7**–**9**) and alkyl acetates (**10**–**12**) are far from being innocuous compounds: all of them are highly volatile, some of them even being gases under standard conditions. The alkyl acetates are highly flammable and form explosive mixtures with air, but especially in the case of chloride ILs it is important to exercise extreme care: the alkyl chlorides formed upon beta-irradiation are potentially toxic, mutagenic, and carcinogenic compounds! CAUTION!!

Future work will now target the observed degradation mechanisms and delve into the "chemistry" of the "physical treatment" method of beta-irradiation. Open questions are, for instance, the regioselectivity of bond cleavages. Especially the quite selective *N*-dealkylation seems attractive from a synthesis point of view as a "chemical-free" alternative to existing *N*-dealkylation/*N*-demethylation procedures (Rosenau et al. 2004). Moreover, the source of protons and electrons required for the reduction of the C–C double bond in imidazolium needs to be clarified, as well as the role of water (traces) in the system. These mechanistic studies are a part of a larger project addressing the system imidazolium ILs/cellulosic pulp under beta-irradiation, for which a covalent fixation of nitrogen in the pulp has been shown (Jusner et al. 2023), while the underlying chemical structures still need to be identified.

Our findings emphasize the importance of considering the degradation of ILs in biorefinery setups involving beta-irradiation, and we hope that our studies contribute to a deeper understanding of the interactions between ionic liquids, beta-irradiation, and lignocellulosic matter, which appear to be more complex and challenging than previously thought.

Acknowledgments We would like to thank the University of Natural Resources and Life Sciences, Vienna (BOKU), the BOKU doctoral school "Advanced Biorefineries: Chemistry & Materials" (ABC&M), and the County of Lower Austria for their financial support through the framework of the Austrian Biorefinery Center Tulln (ABCT-II). The financial support by the GFF Gesellschaft für Forschungsförderung Niederösterreich m.b.H. (A.F.L. and H.H., project LSC20-002) is gratefully acknowledged. We thank the NMR Center at the University of Vienna for the measurements of the gaseous/low-boiling analytes.

Authors' contributions All authors contributed to the study's conception and design. Material preparation, data collection and analysis were performed by all authors. The first draft of the manuscript was written by T.R. All authors commented on previous versions and read and approved the final manuscript.

Funding Open access funding provided by University of Natural Resources and Life Sciences Vienna (BOKU). The authors would like to thank the University of Natural Resources and Life Sciences, Vienna (BOKU), the BOKU doctoral school "Advanced Biorefineries: Chemistry & Materials" (ABC&M), and the County of Lower Austria for their financial support through the framework of the Austrian Biorefinery Center Tulln (ABCT-II). The financial support by the GFF Gesellschaft für Forschungsförderung Niederösterreich m.b.H. (A.F.L. and H.H., project LSC20-002) is gratefully acknowledged.

Data availability No datasets were generated or analysed during the current study.

Code availability Not applicable.

Declarations

Ethics approval Not applicable.

Consent to participate Not applicable.

Consent for publication All authors agreed to the publication in the submitted form.

Competing interests The authors declare no competing interests.

References

Afonso J, Mezzetta A, Marrucho IM, Guazzelli L (2023) History repeats itself again: Will the mistakes of the past for ILs be repeated for DESs? From being considered ionic liquids to becoming their alternative: the unbalanced turn of deep eutectic solvents. Green Chem 25:59–105

Aki SN, Mellein BR, Saurer EM, Brennecke JF (2004) High-pressure phase behavior of carbon dioxide with imidazolium-based ionic liquids. J Phys Chem B 108:20355–20365

Amini E, Valls C, Roncero MB (2021) Ionic liquid-assisted bioconversion of lignocellulosic biomass for the development of value-added products. J Cleaner Prod 326:129275

Barbini S, Jaxel J, Karlström K, Rosenau T, Potthast A (2021a) Multistage fractionation of pine bark by liquid and supercritical CO2. Bioresource Technol 341:125862

Barbini S, Sriranganadane D, España Orozco S, Kabrelian A, Karlström K, Rosenau T, Potthast A (2021b) Tools for bark biorefineries: Studies towards improved characterization of wood extractives by combining supercritical fluid chromatography and high-temperature GCMS. ACS Sust Chem Engin 9(3):1323–1332

Beaumont M, König J, Opietnik M, Potthast A, Rosenau T (2017) Drying of a cellulose II gel: effect of physical modification and redispersibility in water. Cellulose 24(3):1199–1209

Beaumont M, Winklehner S, Veigl S, Mundigler N, Gindl-Altmutter W, Potthast A, Rosenau T (2020) Wet esterification of never-dried cellulose: a simple process to surface-acetylated cellulose nanofibers. Green Chem 22(17):5605–5609

Beaumont M, Tardy BL, Reyes G, Koso TV, Schaubmayr E, King AWT, Jusner P, Dagastine RR, Potthast A, Rojas OJ, Rosenau T (2021) Assembling native elementary cellulose nanofibrils via a reversible and regioselective surface functionalization. J Amer Chem Soc 143(41):17040–17046

Becker M, Zweckmair T, Forneck A, Rosenau T, Potthast A, Liebner F (2013) Evaluation of different derivatisation approaches for GC/MS analysis of carbohydrates in complex matrices of biological and synthetic origin. J Chromatogr A 1281:115–126

Blanchard LA, Gu Z, Brennecke JF (2001) High-pressure phase behavior of ionic liquid/CO2 systems. J Phys Chem B 105:2437–2444

Böhmdorfer S, Oberlerchner JS, Fuchs C, Rosenau T, Grausgruber H (2018) Profiling and quantification of grain anthocyanins in purple pericarp × blue aleurone wheat crosses by high-performance thin-layer chromatography and densitometry. Plant Methods 14(29):2–15

Bouchard J, Methot M, Jordan B (2006) The effects of ionizing radiation on the cellulose of wood-free paper. Cellulose 13:601–610

Brandt A, Erickson JK, Hallett JP, Murphy RJ, Potthast A, Ray M, Rosenau T, Schrems M, Welton T (2012) Ionic liquid pretreatment of pine wood chips for reduced energy input during grinding. Green Chem 14(4):1079–1085

Cappiello A, Famiglini G, Mangani F, Palma P (2001) New trends in the application of electron ionization to liquid chromatography—mass spectrometry interfacing. Mass Spectrometry Rev 20(2):88–104

Croitoru C, Patachia S, Doroftei F, Parparita E, Vasile C (2014) Ionic liquids influence on the surface properties of electron beam irradiated wood. Appl Surf Sci 314:956–966

Croitoru C, Patachia S (2016) Long-chain alkylimidazolium ionic liquid functionalization of cellulose nanofibers and their embedding in HDPE matrix. Int J Polym Sci 4:1–9

Duarte CL, Ribeiro MA, Oikawa H, Mori MN, Napolitano CM, Galvao CA (2012) Electron beam combined with hydrothermal treatment for enhancing the enzymatic convertibility of sugarcane bagasse. Radiat Phys Chem 81:1008–1011

Dubey KB, Pujari PK, Ramnani SP, Kadam RM, Sabharwal S (2004) Microstructural studies of electron beam-irradiated cellulose pulp. Radiat Phys Chem 69:395–400

Ehrhardt A, Miyazaki K, Sato Y, Hori T (2005) Modified polypropylene fabrics and their metal ion sorption role in aqueous solution. Appl Surf Sci 252:1070–1075

Ekman K, Eklund V, Fors J, Huttunen JI, Mandell L, Selin JF, Turunen OT (1984) Regenerated cellulose fibres from cellulose carbamate solutions. Lenzinger Ber 57:38–40

Ershov BG (1998) Radiation-chemical degradation of cellulose and other polysaccharides. Russ Chem Rev 67:154–196

Frisch MJ, Trucks GW, Schlegel HB, Scuseria GE, Robb MA, Cheeseman JR, Scalmani G, Barone V, Petersson GA, Nakatsuji H, Li X, Caricato M, Marenich A, Bloino J, Janesko BG, Gomperts R, Mennucci B, Hratchian H P, Ortiz J V, Izmaylov A F, Sonnenberg J L, Williams-Young D, Ding F, Lipparini F, Egidi F, Goings J, Peng B, Petrone A, Henderson T, Ranasinghe D, Zakrzewski VG, Gao J, Rega N, Zheng G, Liang W, Hada M, Ehara M, Toyota K, Fukuda R, Hasegawa J, Ishida M, Nakajima T, Honda Y, Kitao O, Nakai H, Vreven T, Throssell K, Montgomery Jr. JA, Peralta JE, Ogliaro F, Bearpark M, Heyd J J, Brothers E, Kudin KN, Staroverov V N, Keith T, Kobayashi R, Normand J, Raghavachari K, Rendell A, Burant J C, Iyengar S S, Tomasi J, Cossi M, Millam JM, Klene M, Adamo C, Cammi R, Ochterski JW, Martin RL, Morokuma K, Farkas O, Foresman JB, Fox DJ (2016) Gaussian 09, Revision D.01, Gaussian, Inc., Wallingford CT, 2016

Hao Y, Peng J, Ao Y, Li J, Zhai M (2012) Radiation effects on microcrystalline cellulose in 1-butyl-3- methylimidazolium chloride ionic liquid. Carbohydr Polym 90(4):1629–1633

Henniges U, Okubayashi S, Rosenau T, Potthast A (2012) Irradiation of cellulosic pulps: understanding its impact on cellulose oxidation. Biomacromol 13(12):4171–4178

Henniges U, Hasani M, Potthast A, Westman G, Rosenau T (2013) Electron beam irradiation of cellulosic materials – opportunities and limitations. Materials 6(5):1584–1598

Hosoya T, Bacher M, Potthast A, Elder T, Rosenau T (2018) Insights into degradation pathways of oxidized anhydroglucose units in cellulose by β-alkoxy-elimination – a combined theoretical and experimental approach. Cellulose 25(7):3797–3814

Iller E, Kukielka A, Stupinska H, Mikolajczyk W (2002) Electron-beam stimulation of the reactivity of cellulose pulps for production of derivatives. Radiat Phys Chem 63:253–257

Jusner P, Sulaeva I, Schiehser S, Potthast K, Tischer A, Barbini S, Potthast A, Rosenau T (2023) β-Irradiation in the presence of 1,3-dialkylimidazolium ionic liquids causes covalent cellulose derivatization with simultaneous nitrogen incorporation. Cellulose 30(17):10551–10558

Jusri NAA, Azizan A, Zain ZSZ, Rahman MFA (2019) Effect of electron beam irradiation and ionic liquid combined pretreatment method on various lignocellulosic biomass. Key Engin Mat 797:351–358

Jutz F, Andanson JM, Baiker A (2011) Ionic liquids and dense carbon dioxide: a beneficial biphasic system for catalysis. Chem Rev 111:322–353

Kazarian SG, Briscoe BJ, Welton T (2000) Combining ionic liquids and supercritical fluids: in situ ATR-IR study of CO_2 dissolved in two ionic liquids at high pressures. Chem Comm 2047–2048

Keskin S, Kayrak-Talay D, Akman U, Hortaçsu Ö (2007) A review of ionic liquids towards supercritical fluid applications. J Supercrit Fluids 43:150–180

Kimura A, Nagasawa N, Shimada A, Taguchi M (2016) Crosslinking of polysaccharides in room temperature ionic liquids by ionizing radiation. Radiat Phys Chem 124:130–134

Korntner P, Hosoya T, Dietz T, Eibinger K, Reiter H, Spitzbart M, Röder T, Borgards A, Kreiner W, Mahler AK, Winter H, French AD, Henniges U, Potthast A, Rosenau T (2015) Chromophores in lignin-free cellulosic materials belong to three compound classes. Cellulose 22(2):1053–1062

Kumakura M, Kaetsu I (1983) Effect of radiation pretreatment of bagasse on enzymatic and acid hydrolysis. Biomass 3:199–208

Liebner F, Ebner G, Becker E, Potthast A, Rosenau T (2010) Thermal aging of 1-alkyl-3-methylimidazolium ionic liquids and its effect on dissolved cellulose. Holzforschung 64:161–166

Märk TD, Dunn GH (2013) Electron impact ionization. Springer Science & Business Media

Martinez AS (2023) Novel strategies for extraction and synthesis via combination of supercritical carbon dioxide and ionic liquids. PhD thesis. Vienna University of Technology

Meng X, Wang Y, Conte AJ, Zhang S, Ryu J, Wie JJ, Pu Y, Davison BH, Yoo CG, Ragauskas AJ (2023) Applications of biomass-derived solvents in biomass pretreatment – strategies, challenges, and prospects. Biores Technol 368:128280

Mirsaleh-Kohan N, Robertson WD, Compton RN (2008) Electron ionization time-of-flight mass spectrometry: Historical review and current applications. Mass Spectrometry Rev 27(3):237–285

Mora-Pale M, Meli L, Doherty TV, Linhardt RJ, Dordick JS (2011) Room temperature ionic liquids as emerging solvents for the pretreatment of lignocellulosic biomass. Biotechnol Bioeng 108(6):1229–1245

Nishiyama Y, Wada M, Hanson BL, Langan P (2010) Time-resolved X-ray diffraction microprobe studies of the conversion of cellulose I to ethylenediamine-cellulose I. Cellulose 17(4):735–745

Quesada-Salas MC, Vuillemin ME, Sarazin C, Husson E (2022) Ionic liquids for biomass biotransformation. In: Lozano P (ed) Biocatalysis in green solvents. Academic Press, pp 257–297

Qin L, Li WC, Zhu JQ, Liang JN, Li BZ, Yua YJ (2015) Ethylenediamine pretreatment changes cellulose allomorph and lignin structure of lignocellulose at ambient pressure. Biotechnol Biofuels Bioprod 8:174

Rosenau T, Hofinger A, Potthast A, Kosma P (2004) A general, selective high-yield N-demethylation procedure for tertiary amines by solid reagents in a convenient column chromatography-like setup. Org Lett 6(4):541–544

Roy R, Rahman MS, Raynie DE (2020) Recent advances of greener pretreatment technologies of lignocellulose. Curr Res Green Sust Chem 3:100035

Roy S, Chundawat SPS (2023) Ionic liquid-based pretreatment of lignocellulosic biomass for bioconversion: a critical review. Bioenergy Res 16(1):263–278

Saeman JF, Millet MA, Lawton EJ (1952) Effect of high energy cathode-rays on cellulose. Ind Eng Chem 44:2848–2852

Shin SJ, Sung YJ (2008) Improving enzymatic hydrolysis of industrial hemp (Cannabis sativa L.) by electron beam irradiation. Rad Phys Chem 77:1034–1038

Stolze K, Udilova N, Rosenau T, Hofinger A, Nohl H (2003) Synthesis and characterization of EMPO-derived 5,5-disubstituted 1-pyrroline N-oxides as spin traps forming exceptionally stable superoxide spin adducts. Biol Chem 384(3):457–500

Sulaeva I, Hettegger H, Bergen A, Rohrer C, Rosenau T, Potthast A (2020) Fabrication of bacterial cellulose-based wound dressings with improved performance by impregnation with alginate. Mat Sci Engin C 110:110619

Tu WC, Hallett JP (2019) Recent advances in the pretreatment of lignocellulosic biomass. Curr Opinion Green Sust Chem 20:11–17

Yokota S, Kitaoka T, Opietnik M, Rosenau T, Wariishi H (2008) Synthesis of gold nanoparticles for in situ conjugation with structural carbohydrates. Angew Chem Int Ed Engl 47:9866–9869

Zhang S, Xu T, Zhang N, Liu J, Lin Q, Chen J, Du H, Si C (2021) Green and sustainable preparation of cellulose nanocrystals. China Pulp Paper 40(9):93–102

Zweckmair T, Hettegger H, Abushammala H, Bacher M, Potthast A, Laborie MP, Rosenau T (2015) On the mechanism of the unwanted acetylation of polysaccharides by 1,3-dialkylimidazolium acetate ionic liquids. Part 1: analysis, acetylating agent, influence of water, and mechanistic considerations. Cellulose 22(6):3583–3596